Plasmonic resonance shift for various nanodevice geometries

David A. French[1], Stephen J. Bauman[2], Ahmad Darweesh[2], Desalegn Debu[1], Pijush K. Ghosh[1], Joseph B. Herzog[1,2]
[1]Department of Physics, University of Arkansas; [2]Department of Microelectronics and Photonics, University of Arkansas

ABSTRACT

Plasmonic nanodevices are metallic structures that exhibit plasmonic effects when exposed to light, causing scattering and enhancement of that light. These plasmons makes it possible for light to be focused below the diffraction limit. Dark-field spectroscopy has been used to capture the scattering spectra of these structures in order to examine the scattering and resonant frequencies of the plasmons provided by the devices. The geometries of the devices change which wavelengths of light are most readily able to couple to the device, resulting in a change in the wavelength of the scattered light. A variety of device geometries and configurations will be studied, including nanodiscs, nanowires, and plasmonic gratings, along with double-width nanogap plasmonic gratings. These new structures will have features below the fabrication limit of electron-beam lithography, i.e. sub-10 nanometer features. The polarization dependencies of these resonance modes are investigated as well. A relation between device geometry and wavelength will be drawn; in effect, this will allow the selection of geometry of the fabricated device based on the desired wavelength of light to be scattered. Preliminary Raman spectroscopy will also be performed in order to study the device response and usefulness for surface-enhanced Raman spectroscopy.

Keywords: Dark-field, plasmonic, spectroscopy, grating

1. INTRODUCTION

When metallic nanodevices are exposed to light they exhibit a plasmonic response based on the wavelength of the incoming light and the geometry of the device[1-3]. The plasmon is an oscillation of charge in the device, which itself creates a local oscillating electric field or light. This scattering of light has numerous applications, including improved photovoltaics[4-6], surface-enhanced Raman spectroscopy[7-9], and other uses such as SPASERs[10-12].

This paper attempts to draw a relationship between the geometry of the nanodevice and the resonance peak. This resonance peak refers to the wavelength of light which is most easily scattered by the device. This has been studied by other papers for other devices, including nanodiscs[13], nanowires[14-16], and nanospheres[17]. In this paper, the device geometry of primary interest is a grating. Gratings have been of interest due to the controllable nature of the wire width, period, and material, thereby changing the characteristics of the grating. This makes them desirable for numerous applications, such as sensing and emission of desired wavelengths[18]. Of special interest in this paper is the dual-width nanogap grating, notable for the different wire widths. This results in multiple resonance peaks for each grating.

2. FABRICATION

The nanostructures examined in this work are gold (Au) nanostructures. Each device was fabricated from on a silicon substrate with a 100 nm thermally-grown silicon oxide layer with standard electron beam lithography (EBL). First a thin layer of polymethyl methacrylate electron beam resist was deposited via spin-coating. Next, designs were patterned into the electon beam resist using an electron beam, and then gold was deposited into the developed electron beam resist after development. In order to create the grating, a variation of the self-aligned technique was used[19]. The gratings studied in

this paper were double-width nanogap plasmonic gratings. This type of grating has alternating widths of wires with nanoscale gaps in between as shown in figure 1. The self-aligned technique is what makes these gaps possible. These gratings had fixed small wire widths of w = 100 nm and the period of the plasmonic grating was designed to be P = 230 nm, 300 nm, and 400 nm. Figure 1 shows an image taken with a scanning electron microscope (SEM) of the plasmonic grating with a period of 400 nm. The gap width of this grating varies in size along the length of the nanowires but has an average value of 8 nm. A variation of the self-aligned technique called nanomasking has been shown to make nanogap plasmonic gratings. Bauman et al. describe the full details of this fabrication method that requires two lithography steps[20]. He the method is briefly described. For this work the first lithography step used EBL to patterns a design into a layer of PMMA on a silicon substrate which is then developed in order to create a trough in which to deposit gold. On top of this gold is deposited a layer of chromium. When the chromium layer is exposed to air it oxidizes and expands. The process is repeated but the expanded chromium oxide layer provides a mask beneath which gold cannot be deposited. The chrome oxide layer is then removed with a wet etching process, which leaves side by side gold structures with a nanoscale gap in between. For these gratings, the small wires were patterned first, then the larger wires were deposited. The chromium mask resulted in nanogaps between the wires.

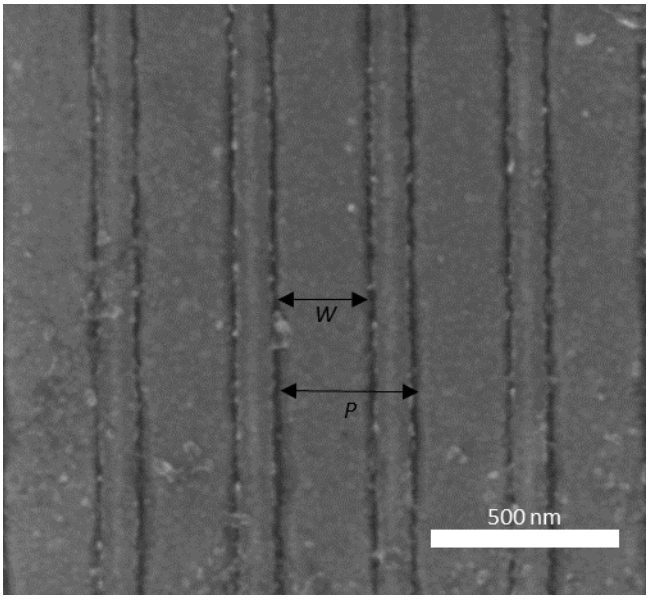

Figure 1. SEM image of double-width nanogap plasmonic grating. The main wire (W) varies by grating, along with the period P. The smaller wire (w) has a fixed width of 100 nm. The period P changes between gratings. This image is of P=400 nm

3. METHODS

3.1 Experimental Methods

Once the gratings were fabricated and imaged by the SEM they were subjected to dark-field spectroscopy. A diagram of the optical setup is shown in figure 2.

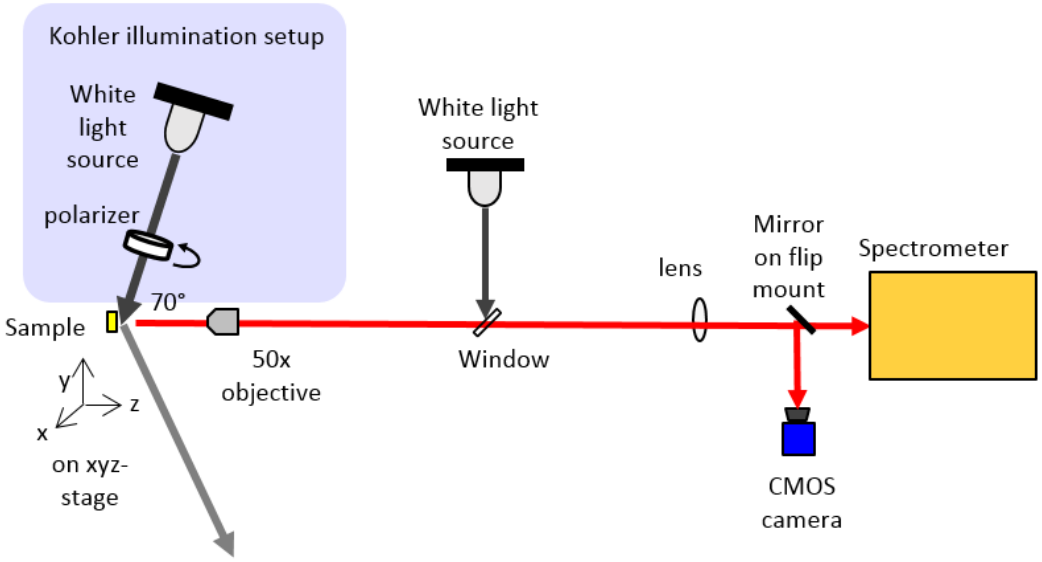

Figure 2. Optical Schematic. Light from a white light source is passed through a linar polarizer and strikes the sample at an incident angle of 70°. The majority of the light is reflected away and the scattered light is collected by the microscope objective (*NA* = 0.55) and sent to either the CMOS camera or the CCD spectrometer after a 200 mm focal length lens. A removable window allows for bright-field imaging of the sample as well.

The optical setup design allows for both bright-field and dark-field imaging of samples. Bright-field imaging allows for colored images of the sample and assists in alignment. Dark-field imaging is used to gather the scattering spectrum. For dark-field, white light from a halogen bulb is sent through a Kohler illumination system with a linear polarizer then to the sample. The majority of the reflected light is ignored while a portion of the scattered light is collected by the 50x microscope objective (NA = 0.55, f = 200 mm). For measuring spectra, the scattered light is then analyzed by a Princeton Instruments InSight:100B spectrometer system with a PIXIS 100B CCD image sensor. An optional flip mount mirror allows for the light to be captured by a CMOS camera, resulting in color images of the samples. Example images of the gratings under both bright-field and dark-field microscopy by this CMOS camera are in figure 3. The system can be changed between dark-field to bright-field imaging by inserting the removable window and turning off the dark-field light source.

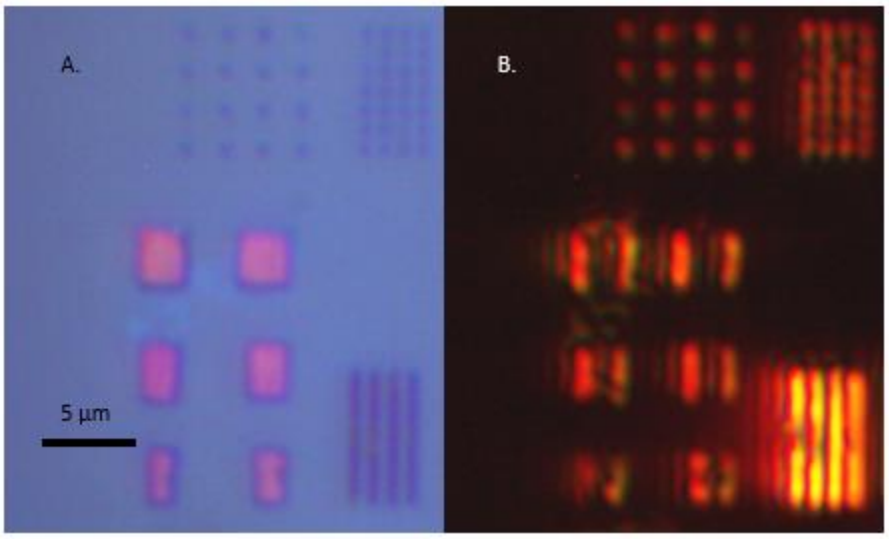

Figure 3. Bright-field (A) and dark-field (B) images of samples. Various nanostructures are fabricated on one chip to save cost. The six purple rectangles in the lower center of (A) are the studied gratings. The gratings closer to the bottom of the image has a narrower width for the main wire and a smaller period. (B) shows dark-field image of the same region. Both images are taken with the CMOS camera.

For this study the spectrometer used a blazed reflection grating of 150 grooves/mm with a blaze angle of 800 nm, which was set at a center wavelength of 750 nm. The CCD was exposed to the scattered light for 5000 ms and 100 exposures were averaged together in order to reduce signal noise as much as possible.

4. RESULTS

The dark-field spectrum was calculated from various measured spectrum, and the resulting data from each grating is plotted in figure 4A. This figure is a waterfall plot, shows that in general the spectra for the various gratings are very similar. The spectra are normalized to show only the differences in the peak position, not any difference in intensity. There are two peaks with each spectrum, likely due to the alternating wire design of the system. Each wire should generate its own resonance peak. These resonance peaks change with the size of the wire, as shown should happen in previous works[21]. There is a noticeable shift in both the primary and secondary peak wavelengths, although the secondary shift is not as drastic. With additional grating sizes it should be quite simple to create an equation which allows for the prediction of the resonance peak based on the grating. We believe that our system is currently detecting a large amount of background scattering; this could be altering the accuracy of our results. Future goals of this project will work towards minimizing these unwanted signals by adding irises to the Kohler illumination system.

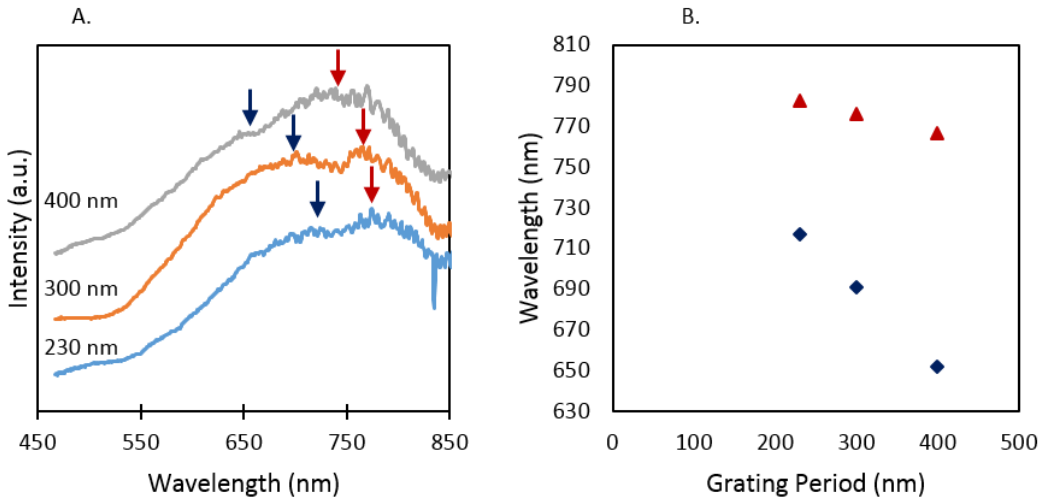

Figure 4. A. Waterfall plot of dark-field spectra of gratings. The arrows show the locations of the two peaks for each grating. B. Peak wavelength plotted for the three grating periods (*P*). The diamonds show the lower wavelength peaks while the triangles show the secondary peaks.

5. CONCLUSION AND FUTURE WORK

There is a relationship between the grating geometry and the resonance peak of the grating. Dark-field spectroscopy has been used to show that the resonance peak shifts as the large wire width changes. With additional trials, a relation can be drawn between the geometry of the grating and the scattering peak of the device. In the future, not only will the grating main wire change, but the other specifications will as well, such as small wire width, height, and gap width. These tests will allow the creation of gratings designed to scatter certain wavelengths of light. In addition, computer simulations will be performed for these gratings to test the expected response for Raman spectroscopy. Finally, future work will also work towards optimizing our optical system by reducing background signals.

ACKNOWLEDGEMENTS

The authors would like to acknowledge the University of Arkansas Graduate School for providing travel funding for this conference through the Doctoral Travel Grant. We would also like to thank the following people at the University of Arkansas for their support: Brandon Rogers, Richard Penhallegon, Mourad Benemara, Greg Forcherio, and Dr. Keith Roper. Funding for this research has been provided by the University of Arkansas Physics Department in the Fulbright College of Arts and Sciences as well as the Arkansas Biosciences Institute.

REFERENCES

[1] Aydin, K., Ferry, V., Briggs, R, and Atwater, H.., "Broadband polarization-independent resonant light absorption using ultrathin plasmonic super absorbers" Nature Communications, 2(517), (2011)

[2] Mock, J., Barbic, M., Smith, D., Schultz, D., and Schultz, S., "Shape effects in plasmon resonance of individual colloidal silver nanoparticles" J. Chem. Phys. 116, 6755 (2002)

[3] Lee, K. and El-Sayed, M., "Gold and Silver Nanoparticles in Sensing and Imaging: Sensitivity of Plasmon Response to Size, Shape, and Metal Composition" J. Phys. Chem. B, 110 (39), 19220–19225 (2006)

[4] Atwater, H. and Polman, A., "Plasmonics for improved photovoltaic devices" Nature Materials, 9, 205–213 (2010)

[5] Mubeen, S., Lee, J., Lee, W., Singh, N., Stucky, G., and Moskovits, M., "On the Plasmonic Photovoltaic" ACS Nano, 8 (6), pp 6066–6073 (2014)

[6] Ferry, V., Munday, J., and Atwater H., "Design Considerations for Plasmonic Photovoltaics" Advanced Materials, 22(43) 4794-4808 (2010)

[7] Sharma, B., Frontiera, R., Henry, A., Ringe, E., and Van Duyne, R., "SERS: Materials, applications, and the future" Materials Today, 15(1-2), 16-25 (2012)

[8] Alvarez-Puebla, R., Cui, B., Bravo-Vasquez, J., Veres, T., and Fenniri, H., "Nanoimprinted SERS-Active Substrates with Tunable Surface Plasmon Resonances" J. Phys. Chem. C, 111 (18), 6720–6723 (2007)

[9] Dornhaus, R., Benner, R., Chang, R., and Chabay, I., "Surface plasmon contribution to SERS" Surface Science 101(1-3), 367-373 (1980)

[10] Noginov, M., Zhu1, G., Belgrave, A., Bakker, R., Shalaev, V., Narimanov, E., Stout, S., Herz, E., Suteewong, T., and Wiesner, U., "Demonstration of a spaser-based nanolaser" Nature 460, 1110-1112 (2009)

[11] Zheludev, N., Prosvirnin, S., Papasimakis, N., and Fedotov, V., "Lasing spaser" Nature Photonics 2, 351 - 354 (2008)

[12] Stockman, M., "The spaser as a nanoscale quantum generator and ultrafast amplifier" Journal of Optics 12(2), (2010)

[13] Langhammer, C., Kasemo, B., and Zorić, I., "Absorption and scattering of light by Pt, Pd, Ag, and Au nanodisks: Absolute cross sections and branching ratios" J. Chem. Phys. 126, 194702 (2007)

[14] Podolskiy V., Sarychev, A., Narimanov, E., and Shalaev, V., "Resonant light interaction with plasmonic nanowire systems" Journal of Optics A, 7(2), (2005)

[15] Ditlbacher, A., Hohenau, A., Wagner, D., Kreibig, U., Rogers, M., Hofer, F., Aussenegg, F., and Krenn, F., "Silver Nanowires as Surface Plasmon Resonators" Physical Review Letters 95 (257403), (2005)

[16] Dorfmüller, J., Vogelgesang, R., Khunsin, W., Rockstuhl, C., Etrich, C., and Kern, K., "Plasmonic Nanowire Antennas: Experiment, Simulation, and Theory" Nano Letters, 10 (9), 3596–3603 (2010)

[17] Sha, W., Choy, W., Liu, Y., and Chew, W., "Near-field multiple scattering effects of plasmonic nanospheres embedded into thin-film organic solar cells" Applied Physics Letters 99, 113304 (2011)

[18] Baba, W., Aoki, N., Shinbo, K., Kato, K., and Kaneko, F., "Grating-Coupled Surface Plasmon Enhanced Short-Circuit Current in Organic Thin-Film Photovoltaic Cells" ACS Applied Materials and Interfaces, 3(6), 2080–2084 (2011)

[19] Fursina, A., Lee, S., Sofin, R., Shvets, I., and Natelson, D., "Nanogaps with very large aspect ratios for electrical measurements", Appl. Phys. Lett., 92(11),113102-1-113102-3 (2008)

[20] Bauman, S., Novak, E., Debu, D., Natelson, D., and Herzog, J. "Fabrication of Sub-Lithography-Limited Structures via Nanomasking Technique for Plasmonic Enhancement Applications" IEEE Transactions on Nanotechnology, 14(5) 790-793 (2015)

[21] Xu, Q., Bao, J., Capasso, F., Whitesides, G., "Surface Plasmon Resonances of Free-Standing Gold Nanowires Fabricated by Nanoskiving" Angewandte Chemie International Edition, 45(22) 3631-3635 (2006)